

# One-rank interaction kernel of the two-nucleon system for medium and high energies

*S. G. Bondarenko, V. V. Burov, W.-Y. Pauchy Hwang<sup>+</sup>, E. P. Rogochaya<sup>1)</sup>*

*Joint Institute for Nuclear Research, 141980 Dubna, Moscow region, Russia*

*<sup>+</sup>National Taipei University, Taipei 106, Taiwan*

Submitted 22 April 2008

A new version of the separable kernel of the nucleon-nucleon interaction in the Bethe-Salpeter approach is presented. The phase shifts are fitted to recent experimental data for singlet and uncoupled triplet partial waves of the neutron-proton scattering with total angular momenta  $J = 0, 1$ . The results are compared with other model calculations.

PACS: 11.10.St, 11.80.Et, 13.75.Cs

**1. Introduction.** The relativistic description of the interaction between two nucleons can be carried out using the Bethe-Salpeter (BS) equation [1]. The BS formalism allows a covariant description of various reactions including electromagnetic ones. The BS approach with the separable kernel of interaction (as a relativistic analogue of the Lippmann-Schwinger equation with the separable potential [2, 3]) demonstrates a good description of electromagnetic processes with the deuteron (such as the elastic lepton-deuteron scattering, deuteron electro- and photodisintegration) and light nuclei (deep inelastic scattering of leptons), see the review [4] and references therein. For instance, the BS formalism facilitates analysis of the role of  $P$  waves (negative energy partial-wave components of the BS amplitude) in the electromagnetic properties of the deuteron and its comparison with the nonrelativistic treatment [5]. Furthermore, the covariant BS approach makes it possible to analyze off-mass-shell effects and contributions of the relativistic two-body currents.

The consistency of the consideration of the deuteron breakup reactions demands the final state interaction (FSI) between the outgoing nucleons to be taken into account. To introduce the FSI of the final  $np$  pair the BS equation for continuous state should be solved. These calculations were performed in the paper [6] for the separable kernel of nucleon-nucleon ( $NN$ ) interaction with a relativistic generalization of Yamaguchi functions. The obtained kernel allows one to describe the  $NN$  phase shifts up to laboratory kinetic energy  $T_{\text{Lab}} \sim 0.6 - 0.7$  GeV (for example, the nonrelativistic Bonn potential can be applied up to  $T_{\text{Lab}} \sim 0.35$  GeV). However, when the amplitudes of reactions in a high ener-

gies region are calculated, this type of functions leads to the presence of nonintegrable singularities. Therefore there are many approaches called quasipotential where the two-body Green's function in the BS equation is replaced by a suitable function which allows to reduce the 4-dimensional integral to the 3-dimensional one, like in [7].

We construct a relativistic generalization of the modified Yamaguchi form factors. For scalar nucleons such functions were introduced in [8]. Functions of this type do not contain poles on the real axis of the relative energy. We use them for the description of the proton-neutron scattering in the wide region of  $T_{\text{Lab}}$  (up to 3 GeV). It is necessary when we consider reactions with light nuclei with a high momentum transfer. In particular, the calculations of the  $d(e, e'p)n$  reaction are supposed to be performed for the relativistic energies using the separable functions elaborated in the paper (see, for example, different kinematical conditions in the Table from [9]).

In this work the one-rank kernel of the  $NN$  interaction for singlet and uncoupled triplet partial states of the neutron-proton ( $np$ ) scattering with total angular momenta  $J = 0, 1$  are presented. The paper is organized as follows: in Sec.2 we set out basic formulae of the formalism, in Sec.3 the functions under consideration are described, in Sec.4 we show the scheme of the calculations and results, Sec.5 is devoted to the analysis of the results and the comparison with calculations within other models, and in Sec.6 we summarize the approach.

**2. Basic formulae.** Let us consider the partial-wave decomposed BS equation for the nucleon-nucleon  $T$  matrix in the rest frame of two particles (the square of the total momentum  $s = (p_1 + p_2)^2$  and the relative momentum  $p = (p_1 - p_2)/2$  [ $p' = (p'_1 - p'_2)/2$ ] are de-

<sup>1)</sup>e-mail: rogoch@theor.jinr.ru

finned through the initial  $p_1$ ,  $p_2$  and final  $p'_1$ ,  $p'_2$  nucleons 4-momenta):

$$T_{ll}(p'_0, p'; p_0, p; s) = V_{ll}(p'_0, p'; p_0, p; s) + \frac{i}{4\pi^3} \int dk_0 \int k^2 dk V_{ll}(p'_0, p'; k_0, k; s) \times S(k_0, k; s) T_{ll}(k_0, k; p_0, p; s). \quad (1)$$

Here  $T_{ll}$  is the partial-wave decomposed  $T$  matrix ( $l$  enumerates  $^S L_J^{\rho}$  states for simplicity,  $S$  is the spin of two particles,  $L$  is an orbital momentum, and  $\rho$  spin defines a sign of an energy),  $V_{ll}$  is the interaction kernel,  $E_k = \sqrt{k^2 + m^2}$ ,  $m$  is a nucleon mass. We consider uncoupled partial states, and therefore the  $T$  matrix does not have transitions to different partial states. The two-particle propagator is

$$S(k_0, k; s) = 1 / ((\sqrt{s}/2 - E_k + i\epsilon)^2 - k_0^2). \quad (2)$$

Using the separable anzatz for the one-rank kernel of the  $NN$  interaction

$$V_{ll}(p'_0, p'; p_0, p; s) = \lambda_l(s) g^{[l]}(p'_0, p') g^{[l]}(p_0, p), \quad (3)$$

we obtain the solution of the equation (1) for the  $T$  matrix in the similar separable form:

$$T_{ll}(p'_0, p'; p_0, p; s) = \tau_l(s) g^{[l]}(p'_0, p') g^{[l]}(p_0, p), \quad (4)$$

where

$$\tau_l(s) = 1 / (\lambda_l(s)^{-1} + h_l(s)) \quad (5)$$

with

$$h_l(s) = -\frac{i}{4\pi^3} \int dk_0 \int k^2 dk \frac{(g^{[l]}(k_0, k))^2}{(\sqrt{s}/2 - E_k + i\epsilon)^2 - k_0^2}, \quad (6)$$

and  $\lambda_l$  is a model parametric function. From the normalization condition for the  $T$  matrix in the on-mass-shell form:

$$T_{ll}(s) \equiv T_{ll}(0, \bar{p}; 0, \bar{p}; s) = -\frac{16\pi}{\sqrt{s}\sqrt{s-4m^2}} e^{i\delta_l} \sin \delta_l, \quad (7)$$

where  $\bar{p} = \sqrt{s/4 - m^2} = \sqrt{mT_{\text{Lab}}b/2}$  is the on-mass-shell momentum, the phase shift  $\delta_l$  for the one-rank kernel of interaction is defined as

$$\cot \delta_l(s) = \frac{\text{Re } T_{ll}(s)}{\text{Im } T_{ll}(s)} = -\frac{\lambda_l(s)^{-1} + \text{Re } h_l(s)}{\text{Im } h_l(s)}. \quad (8)$$

We obtain the low-energy scattering parameters expanding the following expression for  $S$  waves into series of  $\bar{p}$ -terms [10]:

$$\bar{p} \cot \delta_l(s) = -1/a_l + \frac{1}{2} \bar{p}^2 r_{0l} + \mathcal{O}(\bar{p}^3). \quad (9)$$

Here the scattering length  $a_l$  and the effective range  $r_{0l}$  are introduced. Since it is clear which partial states are discussed, hereinafter we omit the index  $l$  for simplicity.

**3. One-rank kernel.** We analyze two relativistic generalizations of the Yamaguchi form factors: modified Yamaguchi (MY) functions and modified extended Yamaguchi (MEY) functions.

**3.1. Modified Yamaguchi functions.** For the description of the chosen partial states we use the following covariant expressions:

$$g^{[S]}(p_0, p) = \frac{(p_{c1} - p_0^2 + p^2)}{(p_0^2 - p^2 - \beta^2)^2 + \alpha^4}, \quad (10)$$

$$g^{[P]}(p_0, p) = \frac{\sqrt{-p_0^2 + p^2}}{(p_0^2 - p^2 - \beta^2)^2 + \alpha^4}. \quad (11)$$

The functions are numerated by angular momenta  $L = 0([S]), 1([P])$ . The numerator in  $g^{[S]}$  is introduced to compensate an additional dimension in the denominator to provide the total dimension as  $\text{GeV}^{-2}$ . This form was chosen because at  $p_{c1} = \beta^2$ ,  $\alpha = 0$  we get the function  $g^{[S]}$  in the standard Yamaguchi form [6]. We prefer not to consider the case with the square root in the denominator as it is used in [8] for  $S$  waves to avoid the calculations with cuts on the real axis in  $p_0$  complex plane.

**3.2. Modified extended Yamaguchi functions.** To extend the form of functions with increasing number of parameters we introduce the following  $g$  functions:

$$g^{[S]}(p_0, p) = \frac{(p_{c1} - p_0^2 + p^2)}{(p_0^2 - p^2 - \beta_1^2)^2 + \alpha_1^4} + \frac{C_{12}(p_0^2 - p^2)(p_{c2} - p_0^2 + p^2)^2}{((p_0^2 - p^2 - \beta_2^2)^2 + \alpha_2^4)^2}, \quad (12)$$

$$g^{[P]}(p_0, p) = \frac{\sqrt{-p_0^2 + p^2}}{(p_0^2 - p^2 - \beta_1^2)^2 + \alpha_1^4} + \frac{C_{12} \sqrt{(-p_0^2 + p^2)^3} (p_{c3} - p_0^2 + p^2)}{((p_0^2 - p^2 - \beta_2^2)^2 + \alpha_2^4)^2}. \quad (13)$$

The denominators with  $p_{c1}, p_{c2}, p_{c3}$  are intended for dimension compensation as  $p_{c1}$  for  $g^{[S]}$  in the previous case (10).

**4. Calculations and results.** Using the  $np$  scattering data we analyze the parameters of the separable kernel distinguishing three different cases:

1. There are no sign change in phase shifts or bound state ( $^1P_1$ ,  $^3P_1$  partial states). In this case

Table 1

**Parameters of the one-rank kernel with modified Yamaguchi functions**

	$^1S_0^+$	$^3S_1^+$		$^1P_1^+$	$^3P_0^+$	$^3P_1^+$
$T_{\text{Lab}}^{\text{max}}, \text{ GeV}$	0.999	1.1		1.1	0.999	0.999
$\lambda, \text{ GeV}^2$	-1.0375	-10.004	$\lambda, \text{ GeV}^4$	8.11284	-211.74	11.962
$\alpha, \text{ GeV}$	1.3312	-11.287	$\beta, \text{ GeV}$	0.56487	0.53808	0.58466
$\beta, \text{ GeV}$	0.1	1.3540	$\alpha, \text{ GeV}$	0.2	0.85720	0.2
$p_{c1}, \text{ GeV}^2$	19.229	0.49696				
$s_0, \text{ GeV}^2$	4.0279	4.2020			3.8682	

Table 2

**Parameters of the one-rank kernel with modified extended Yamaguchi functions**

	$^1S_0^+$	$^3S_1^+$		$^1P_1^+$	$^3P_0^+$	$^3P_1^+$
$T_{\text{Lab}}^{\text{max}}, \text{ GeV}$	0.999	1.1		1.1	2.83	0.999
$\lambda, \text{ GeV}^2$	-0.84694	-9.1434	$\lambda, \text{ GeV}^4$	0.054821	-192.60	0.030177
$C_{12}, \text{ GeV}^0$	-8.6404	3.3641	$C_{12}, \text{ GeV}^0$	4.67839	4.9604	-0.39145
$\beta_1, \text{ GeV}$	0.13400	2.6609	$\beta_1, \text{ GeV}$	0.21829	0.71329	0.19951
$\beta_2, \text{ GeV}$	0.92330	0.12501	$\beta_2, \text{ GeV}$	0.20829	0.70329	0.66216
$\alpha_1, \text{ GeV}$	1.4553	2.0808	$\alpha_1, \text{ GeV}$	0.20500	0.70958	0.20000
$\alpha_2, \text{ GeV}$	0.93129	1.6340	$\alpha_2, \text{ GeV}$	0.52835	1.4574	0.32015
$p_{c1}, \text{ GeV}^2$	24.261	189.85	$p_{c3}, \text{ GeV}^2$	0.36868	-1.7576	-117.75
$p_{c2}, \text{ GeV}^2$	-2.1076	3.6688				

$$\lambda_l(s) = \text{const.} \quad (14)$$

This is sufficient for the most of the higher partial waves.

2. One sign change and no bound state ( $^1S_0$ ,  $^3P_0$  partial states). In this case the energy-dependent expression for  $\lambda_l$  is used (see [8] and references therein):

$$\lambda_l(s) = \lambda(s_0 - s). \quad (15)$$

Here the parameter  $s_0$  is introduced to reproduce the sign change in the phase shifts at the position of the experimental value for the kinetic energy  $T_{\text{Lab}}$  where they are equal to zero. It is added to the other parameters of the kernel.

3. One sign change and one bound state ( $^3S_1$  state). In this case in addition to the zero in the phase shifts the  $T$  matrix has a pole at the mass of the bound state  $M_b$ :

$$\det |\tau^{-1}(s = M_b^2)| = 0. \quad (16)$$

To achieve this we set

$$\lambda_l(s) = \lambda \frac{s_0 - s}{s - m_0^2}. \quad (17)$$

The parameter  $m_0$  is chosen to satisfy the condition (see eq. (16) and (17))

$$\lambda^{-1} \frac{M_b^2 - m_0^2}{s_0 - M_b^2} + \text{Re } h(M_b^2) = 0, \quad (18)$$

where  $M_b = (2m - E_b)$  defines the mass of the bound state and  $E_b$  is its energy.

The calculation of the parameters is performed by using the equations (8), (9) and expressions given in previous section to reproduce experimental values for the phase shifts till the maximal laboratory kinetic energy  $T_{\text{Lab}} < T_{\text{Lab}}^{\text{max}}$ , deuteron energy and low-energy scattering parameters. Experimental data for phase shifts are taken from the SAID program (<http://gwdac.phys.gwu.edu>) and for the rest quantities – from [11]. For all states except  $^3P_0$  the  $T_{\text{Lab}}^{\text{max}}$  is chosen to be  $\sim 1$  GeV both for MY and MEY cases and for  $^3P_0$  wave –  $\sim 3$  GeV for MEY case.

Now we find the introduced parameters of the kernel:

1. For  $P$  waves the minimization procedure for the function

$$\chi^2 = \sum_{i=1}^n (\delta^{\text{exp}}(s_i) - \delta(s_i))^2 / (\Delta \delta^{\text{exp}}(s_i))^2 \quad (19)$$

is used. Here the number of experimental points  $n$  depends on the  $T_{\text{Lab}}^{\text{max}}$  value.

2. For  $S$  waves the values of the scattering length  $a$  are also included into the minimization procedure

The low-energy scattering parameters and binding energy for the singlet ( $s$ ) and triplet ( $t$ )  $S$  waves

	$a_s$ , Fm	$r_{0s}$ , Fm	$a_t$ , Fm	$r_{0t}$ , Fm	$E_d$ , MeV
MY	-23.80	2.4	5.43	1.8	2.2246
MEY	-23.74	2.51	5.39	1.73	2.2246
Experiment	-23.748(10)	2.75(5)	5.424(4)	1.759(5)	2.224644(46)

$$\chi^2 = \sum_{i=1}^n (\delta^{\text{exp}}(s_i) - \delta(s_i))^2 / (\Delta\delta^{\text{exp}}(s_i))^2 + (a^{\text{exp}} - a)^2 / (\Delta a^{\text{exp}})^2. \quad (20)$$

The effective range  $r_0$  is calculated through the obtained parameters and compared with the experimental value  $r_0^{\text{exp}}$ . The value of the binding energy  $E_d$  for the case  ${}^3S_1$  is taken into account by introduction of the parameter  $m_0$  in eq.(17).

The calculated parameters of the one-rank kernel with MY and MEY functions and  $T_{\text{Lab}}^{\text{max}}$  are listed in Tables 1 (here the values of  $s_0$  are presented, too) and 2. In Table 3 the calculated low-energy scattering parameters for  $S$  waves are compared with their experimental values.

In Figs.1–5 the results of the phase shifts calcu-

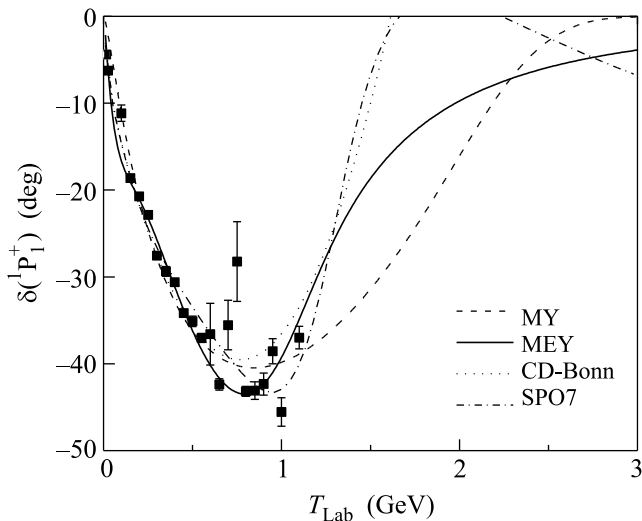


Fig.1. Phase shifts for the  ${}^1P_1^+$  wave. Dashed line corresponds to our parametrization with MY functions, eq.(11); the solid line illustrates the extended case, eq.(13); the dotted and dash-dotted lines describe the CD-Bonn and SP07 calculations, correspondingly

lations are compared with experimental data and two alternative descriptions by CD-Bonn [12] and SP07 [13].

**5. Discussion.** The calculated phase shifts are presented in Figs.1–5 and parameters of the separable

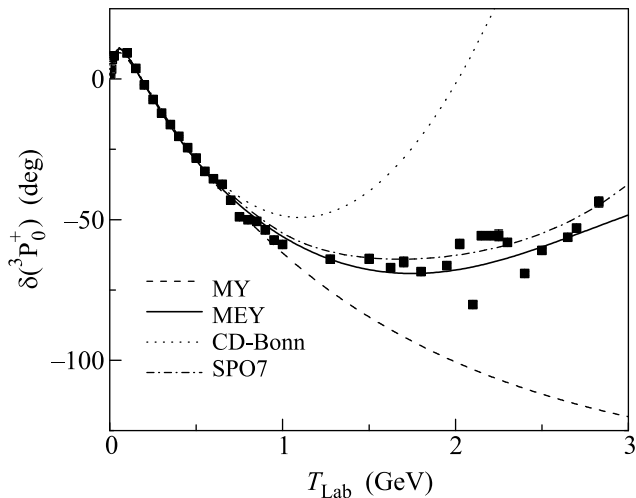


Fig.2. The same as in Fig.1 for the  ${}^3P_0^+$  state

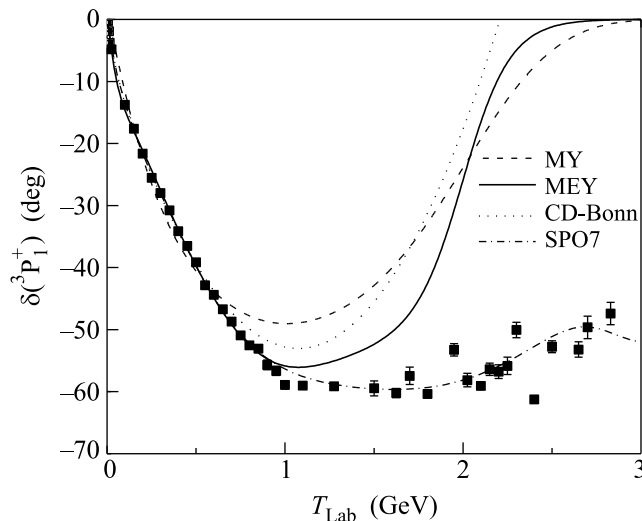


Fig.3. The same as in Fig.1 for the  ${}^3P_1^+$  state

kernel are given in Tables 1–2 (MY case is denoted by the dashed line, MEY one – by the solid line). The calculations with the nonrelativistic CD-Bonn potential (dotted line) and the solution SP07 [13] (dash-dotted line) are included for comparison.

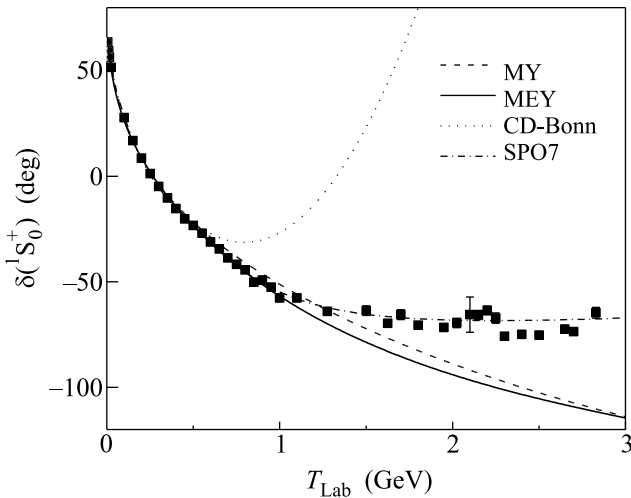


Fig.4. The same as in Fig.1 for the singlet partial state  $^1S_0^+$ , but the description by MY functions is defined by eq.(10) and extended one (MEY) – by eq.(12)

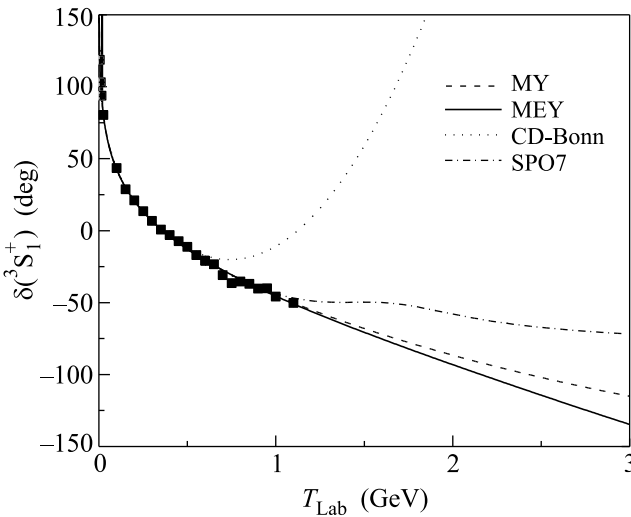


Fig.5. The same as in Fig.4 for the triplet partial state  $^3S_1^+$

We can see in Fig.1 that all the calculations give a reasonable agreement with experimental data up to energy  $T_{\text{Lab}} \sim 1.1$  GeV but at larger energies their behavior becomes different drastically. Note that the CD-Bonn and SP07 results for phase shifts even change sign at  $1.5 < T_{\text{Lab}} < 2.5$  GeV. So we can stress that it is very desirable to obtain more exact determination of experimental data for the  $^1P_1^+$  channel in this energy range. Now keeping in mind that the discrepancies between CD-Bonn, MEY and SP07 calculations at  $T_{\text{Lab}} < 1.2$  GeV are not so large we can trust our calculations in this range of energies.

In Fig.2 we can see that CD-Bonn and MY calculations demonstrate an opposite behavior for  $^3P_0^+$  phase shifts at  $T_{\text{Lab}} > 1$  GeV. The MEY and SP07 calculations give a very good agreement with experimental data in a

wide range of energies  $T_{\text{Lab}} < 3$  GeV. Thus, our model for the kernel of the  $NN$  interaction in the  $^3P_0^+$  channel is acceptable to be used in various relativistic calculations of reactions.

Calculations for the  $^3P_1^+$  channel (see Fig.3) show us that MY, CD-Bonn, and MEY have similar behavior in a wide energy range, but can explain experimental data up to  $T_{\text{Lab}} = 0.55, 0.6$  and  $1.2$  GeV, respectively. The SP07 calculations give a suitable agreement with experimental data up to  $3$  GeV. Thus to explain the data for the  $^3P_1^+$  channel in wider energy range in our approach we need to increase the rank of the separable kernel of the  $NN$  interaction.

Fig.4 demonstrates a close agreement with experimental data for CD-Bonn up to the energy  $T_{\text{Lab}} < 0.6$  GeV, MY and MEY up to  $T_{\text{Lab}} < 1.2$  GeV in the  $^1S_0^+$  channel (note that these calculations give very similar behavior of phase shifts in the wide energy range up to  $3$  GeV). We can conclude that in this case as well as for  $^3P_1^+$  we need to increase the rank of the separable kernel of the  $NN$  interaction. The SP07 calculations describe experimental data for the  $^1S_0^+$  channel up to  $3$  GeV.

Fig.5 for the  $^3S_1^+$  wave shows us that CD-Bonn calculations agree with experimental data up to  $0.6$  GeV. MY, MEY, and SP07 have similar behavior in a wide energy range and explain known experimental data up to  $T_{\text{Lab}} = 1.1$  GeV. It should be noted that calculations of low-energy parameters with MY and MEY form factors give us a reasonable agreement with their experimental values (see Table 1).

**6. Conclusion.** We present the new parametrizations of the separable kernel of the  $NN$  interaction which are adopted for calculations at large energies. As it was expected the MEY functions give a better description of the scattering data than the MY ones. Using the suggested MEY form factors the phase shifts are described in a whole range of measured energies for the following partial states:  $^1P_1^+$ ,  $^3S_1^+$  ( $T_{\text{Lab}} < 1.2$  GeV) and  $^3P_0^+$  ( $T_{\text{Lab}} < 3$  GeV). The phase shifts for the  $^1S_0^+$  and  $^3P_1^+$  partial states can be described in our approach up to  $T_{\text{Lab}} < 1.2$  GeV. To improve an agreement with experimental data up to  $T_{\text{Lab}} < 3$  GeV it is necessary to increase the rank of the separable kernel of the  $NN$  interaction. It is planned to be done in the near future.

We wish to thank our collaborators A.A. Goy, K.Yu. Kazakov, D.V. Shulga, and Y. Yanev for fruitful discussions.

1. E. E. Salpeter and H. A. Bethe, Phys. Rev. **84**, 1232 (1951).

2. L. Mathelitsch, W. Plessas, and W. Schweiger, *Phys. Rev. C* **26**, 65 (1982).
3. J. Haidenbauer and W. Plessas, *Phys. Rev. C* **30**, 1822 (1984).
4. S. G. Bondarenko et al., *Prog. Part. Nucl. Phys.* **8**, 449 (2002).
5. S. G. Bondarenko et al., *Part. Nucl., Lett.* **2**, 270 (2005).
6. S. G. Bondarenko et al., *Part. Nucl., Lett.* **2**, 264 (2005).
7. R. Blankenbecler and R. Sugar, *Phys. Rev.* **142**, 1051 (1966).
8. K. Schwarz, J. Frölich, H. F. Zingl, and L. Streit, *Acta Phys. Austr.* **53**, 191 (1981).
9. S. G. Bondarenko, V. V. Burov, E. P. Rogochaya, and A. A. Goy, *Phys. Atom. Nucl.* **70**, 2054 (2007).
10. H. A. Bethe, *Phys. Rev.* **76**, 38 (1949).
11. O. Dumbrajs et al., *Nucl. Phys. B* **216**, 277 (1983).
12. R. Machleidt, *Phys. Rev. C* **63**, 024001(01) (2001).
13. R. A. Arndt, W. J. Briscoe, I. I. Strakovsky, and R. L. Workman, *Phys. Rev. C* **76**, 025209 (2007).